Fatigue Indicators of Drivers by Using Non-Fatal Abetment Monitoring System

A.Sangeetha[#1], A.Santhiya[*2], K.Santhakumar[#3]

[1,2]Electronics and Communication Engineering, Nandha Engineering College (Autonomous)
Tamilnadu, India
[1]rajkumarsangeetha93@gmail.com
[2]santhiyaec134@gmail.com
[3]Associate professor/ECE
Tamilnadu, India
[3]ecebank@gmail.com

***Abstract*—Driver assistance system helps the driver in the driving process .Designed with a safe Human-Machine interface they should increase car safety and more generally road safety. Physiological signals including eye blinking, ECG, EEG measurement system requires the electrodes to be in contact with human skin. This system remotely detects the signals. The driver Attention monitoring system includes a camera placed on the steering column which is capable of eye tracking. If the driver is not paying attention to the road ahead and a dangerous situation is detected, the system will warn driver by warning sounds. Ultrasonic signals will avoid collision between vehicles moving front. Byusing delicate sensors, this system will able to detect ECG signals through cloth with no contact with skin. To decimate the signal noise, digital signal processing algorithms are used. The essential signals were further analyzed to evaluate the potential criterion for attentiveness and drowsiness determination.**

***Index Terms*—Driver fatigue, electrocardiography (ECG), electroencephalography (EEG), eye blinking, health monitoring, intelligent vehicle, nonintrusive, road safety.**

I. INTRODUCTION

GROWING aging population is a global phenomenon in **recent** decades. The increasing number of elderly car drivers and the prevalence of chronic diseases call for driver assistance systems to monitor the health state of drivers. For medical-assistance systems, the reliable measurement of vital signals such as electroencephalography (EEG) and electrocardiography (ECG) is one of the most important features [1]. ECG and the secondary parameters including heart rate (HR) and heart rate variability (HRV) are key indicators of the cardiac health state. The stressful condition of driving and the possible sudden scenarios on the road, e.g., fatal traffic Accidents, may cause severe effects especially on the drivers with chronic diseases [2]. Therefore, a driver assistance system that can monitor the multiple vital signals during driving is highly desirable for elderly drivers or drivers with chronic diseases

For drivers at all ages, drowsiness is one of the most prevalent root causes of accidents. It leads to nearly 17% of all fatal crashes in recent years based on the data published by the National Highway Traffic Safety Administration [3]. In particular, truck driver fatigue is a factor in 3%–6% of fatal crashes involving large trucks. The term driver fatigue

A number of physiological parameters have been found to indicate the state of fatigue. Eye activity [7], [8], EEG [9], [10], ECG, and HRV [11], [12] are the major physiological indicators used for assessment of sleepiness. Feature extraction was developed based on different types of physiological signals to classify drowsy versus awaken drivers. Therefore, the vital signals (such as ECG, EEG, and eye blinking) are not only indicators of the health state of drivers but also can be used to detect the driver fatigue.

The conventional ECG and EEG systems use Ag/AgCl electrodes with a wet electrolyte. Skin preparation is required be-fore placing the electrodes. For eye activity detection in driving application, video cameras are commonly used to detect the eye-related parameters such as PERCLOS [13] and reopening time [7]. Image processing algorithms and related computation processors are necessary to extract the features from video images. However, few other methods were explored to detect eye activities.

In contrast to the conventional wet electrodes, capacitive electrode (CE) provides an alternative way of surface potential measurement without direct contact with skin. This nonintrusive electrode can sense the bio potentials outside the hair or cloth [14]. A number of devices using CE have been reported for health care with sensors placed on bed [15], chairs [16] and wheelchair [17], exercise assistance [18], and automobiles [1]. ECG or EEG signals can be detected from these systems.

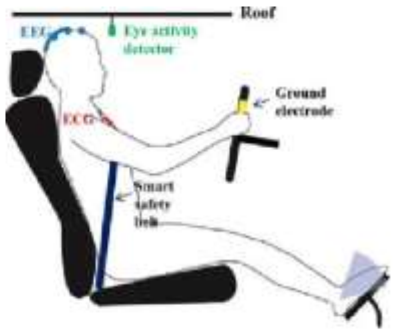

Fig. 1. Driver assistance system.

In the automobile system application, high interface environment (e.g., when engine is on) and severe motion artifacts are unavoidable. Wet electrodes were commonly used to guarantee good contact with skin and prevent relative motion. CEs were also attempted by several groups for unobtrusive ECG measurement [1], [19]–[22]. Large-area metal plates were installed on the steer or car seat as grounding or driven-right-leg (DRL) electrodes to ensure stable signals.

In this study, we developed an innovative in-vehicle nonintrusive driver assistance system that can measure ECG, EEG, and eye-blinking activities in one device (see Fig. 1). Unipolar electrode was adopted to minimize the placement and enhance the simplicity of installation and comfort of drivers. It also provides an easy way to detect the eye activities compared with a video camera. The proposed noncontact vital signal monitoring system can not only monitor the health state of drivers, but also detect driver fatigue. In this paper, details of technology concept and system design were described. Experiments were conducted on a high fidelity driving simulator. It was found that EEG, ECG, and eye-activity signals can be reliably measured by the system. From these, basic medical care functions such as HR monitoring can be accomplished in real time. Moreover, eye features, EEG spectrum, and HRV features from the subjects in alertness and sleepiness states were analyzed to explore the potential algorithm for driver fatigue detection.

II.BACKROUND

A. Skin–Electrode Interface

B. The bio potentials on the skin are generated by the bioelectric activity of organs such as heart and brain, and conducted by neurons. Between the surface bio potentials and the electrodes, there are different layers including stratum corneum, cloth, insulation layer, and air gap. Each of these layers is equivalent to an RC parallel component. The skin–electrode impedance can be calculated by the equivalent model shown in Fig. 2(a). The general total impedance of the skin–electrode interface is [14]

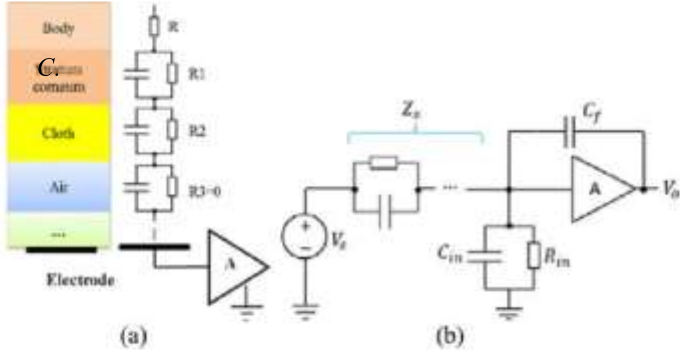

Fig. 2. Equivalent models. (a) Equivalent skin–electrode interface of CEs.

(b) Equivalent circuit of the following analog front end.

B. Specification of In-Vehicle Application

During driving process, drivers keep adjusting the operation of vehicles according to the changing environment. The actual interface between the skin and the electrode change with motion. The impedance of skin–electrode interface is not stable, which will affect the reliability of signal acquisition. When using a small-area electrode, the coupling capacitance during motion can vary from 0.1 to 100 pF. This calls for ultrahigh input impedance of the amplifier to ensure the high sensitivity. The typical input impedance of commercial amplifiers can be up to $10^{15}\Omega/0.2$ pF (i.e., INA116, Texas Instrument, Inc.). It is sufficiently high to acquire the signal but cannot eliminate the influence of the changes in the capacitance of interfaces. One solution is bootstrapping to enhance the input impedance which has been adopted by several groups for capacitive ECG detection [14], [23].

Other than motion artifacts, high interference is also a challenge for application of noncontact physiological monitoring system for automobile applications. During driving, the un-screened environment with high EM interference from vehicle and cellphone can easily immerse the physiological signals. The displacement current induced by the EM field couples to the body and generates both common-mode and differential-mode voltages. DRL circuit and good grounding of body are usually used to reduce the common-mode voltage [1], [22]. However, the DRL circuit requires additional electrodes and wire connection. High CMRR amplifiers and good shielding are also key issues to eliminate the common-mode effects. For differential-mode voltage, highly matched electrodes are required. High input impedance is also desirable to lessen the differential noise [24]. In summary, delicate system design is necessary to implement noncontact vital signal sensing for automobile application.

III. SYSTEM DESIGN

A. System Architecture

Our proposed system adopts unipolar design to simplify the system installation and increase the comfort of drivers. The unipolar pattern was also adopted by Gargiulo *et al.* [25]. The

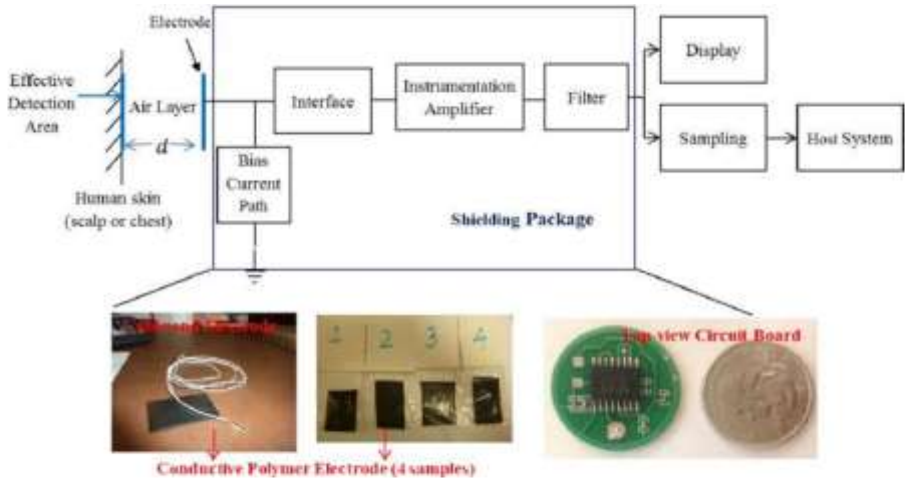

Fig. 3. Block diagram and photos of the noncontact physiological detection sensor.

Advantages and feasibility were approved by Meziane et al [26]. In our design a small conductive plate is used as the electrode with area of 4.5 × 2 cm^2. Another plate Of the same material and size is attached to the steer as the ground connection.

Fig. 3 shows the block diagram and the photo illustrations. The circuit board is as small as a US quarter.

1). Electrode: In the proposed system, metal plate's including stainless steel, soft copper tap and solder mask, are tested as the electrode material. Besides the common metallic electrodes, an appealing type is the conductive polymers which are organic polymers with high electrical conductivity. It features the advantages of polymers to allow for flexible design of electrodes. The electrons in this structure have high mobility when the material is doped by oxidation which removes some of these delocalized electrons. During doping, small fraction silicon atoms are re-placed by electron-rich or electron-poor atoms to create n-type and p-type semiconductors, respectively. In this paper, we evaluate four types of conductive polymers according to the dopants. The conductive-polymer electrodes are flexible and biocompatible, and can be conveniently integrated with clothing.

2).Instrumentation Amplifier: To obtain high input impedance and low noise, an instrumentation amplifier INA116(Texas Instrument, Inc.) Was applied for amplification. The in-put impedance is 10^1 $^5\Omega$/0.2 pF. The CMRR is around 90 dB at 0–1 kHz with the gain of 10 V/V.

1) Bias Current Path: The instrumentation amplifier has the input bias current with a typical value of 3 fA. The bias current path provides an equivalent resistance for the bias current toground to avoid saturation. However, the equivalent parallel reistance can lower the input impedance if not larger than 100 TΩ. Some studies used the reverse current of signal diodes to pro-vide the bias current [35], [36]. In our design, we calculated the

Input resistance and capacitance to the ground according to the actual condition to form a bias path with impedance as 10^1 $^4\Omega$. Then we made the layout dimension based on the calculation strictly.

4) Filter: The frequency components of normal ECG signal ranges from 0.01 to 100 Hz with energy concentrating in 0.5–45 Hz. The major bands of EEG signal range in 0–30 Hz. Therefore, a low pass filter with cut off frequency at 45 Hz is designed to filter out the high-frequency noise including the power line interference. A fourth-order Butterworth filer with the multiple feedback topologies is chosen.

5) Shielding and Grounding: Comparing with the DRL three-electrode circuit, the single-ended circuit has higher noise level and less stability; however, it requires less attachment and causes less distraction to drivers. One compensative method is to reduce the common mode voltage by good shielding and lessen the coupling capacitance between body and ground by use of grounding electrodes. In the design, we found that a thick copper shielding box could reduce the interference significantly. The typical detected signals are shown in Section V.

B. Equivalent Circuit Model

The equivalent circuit model considering the skin–electrode interface is shown in Fig. 2(b). The capacitance of each layer can be computed as $C = \varepsilon_r \varepsilon_0 S/d$, where S is the effective area which is 4.5 × 2 cm^2, and d is the thickness of 0.2–1 mm for the cotton layer (dominant layer). Therefore, the capacitance of the skin–electrode interface is ranging from 8 to 40 pF. The capacitance and the bias resistance form a high pass filer with the cut off frequency at around 0.08 Hz. The transfer function for the circuit model can be expressed as

$$\frac{V_0}{V_s} = \frac{AZ_{in}}{Z_{sb,sc} + Z_{in} + (1-A) j\omega C_f Z_{in} Z_{sb,sc}} \quad .(2)$$

IV. EXPERIMENT

A. Equipment

The experiments were conducted on a high fidelity driving simulator. The simulator consists of a vehicle body with dual and rear view mirrors, six angled projection surfaces, audio systems

Fig. 4. High fidelity driving simulator.

And master control system providing 360° vision to the drivers. The scenarios and driving routes can be designed and loaded into the simulator. Prior to the experiment, normal urban and highway scenarios were developed for driving testing. The driver assistance system was installed as Fig. 1. Fig. 4 shows the driving simulator and a typical scenario.

The driving experience on the simulator was evaluated by a survey. Thirty subjects (8 female and 22 male, age 20–30, average driving experience 4.11 years) participated in the survey by driving the simulator for 15 min and answering a questionnaire. Nine questions were designed to estimate the similarity between driving in the simulator and real environment in terms of the entire driving experience and eight specific aspects such as the feeling of accelerating, distance, collision, etc. The results showed that the driving simulator reasonably well simulated the realistic driving environment based on the feedbacks from the survey.

B. Subjects and Experiment Protocol

Twelve volunteer drivers (nine male and three female) aged 24–30 (26 ± 2.12) years participated in the experiment on the driving simulator. All the participants were recruited from the university and selected as self-evaluated healthy and not addicted to drug or alcohol. Each subject was instructed to drive with his/her normal driving behaviours. Since the driver assistance system can keep monitoring the health state by measuring the vital signals, its performance was verified simultaneously with the experiment of driver fatigue detection.

In the driving simulator, a copper strip detector was attached to the safety handle from the roof, which hung to the side of the driver's head at a distance of around 10 cm. The detector re-motely monitored the bio potentials associated with eye blinking activities [see Fig. 6(a)]. For subjects wearing glasses, the electrode was also attached to the glasses frame. For EEG recording, the electrodes were placed on top of the hair following the 10– 20 international standard of EEG electrode placement [28]. The Fz and Oz channels were adopted as suggested by Khushaba *et al.* and Santamaria and Chiappa [29], [30]. Neither hair was removed, nor coupling gel applied. The electrodes were fixed by a hairband. For ECG recording, the electrode was attached on the chest of drivers through cloth.

Fig. 5. Typical scale results using continuous Wierwille and Ellsworth criteria. 1—class 1, 2—class 2, 3—class 3, 4—class 4, and 5—class 5. (a) Scale results in the morning section. (b) Scale results in the afternoon section.

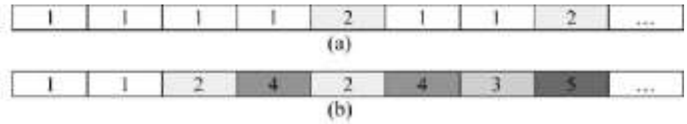

The study involved two experimental sessions in the same day. Each session took 15–20 min. One was conducted in the morning when the subjects were self-evaluated as alert, and

The other was in the afternoon after lunch when the subjects were more possibly drowsy. The ECG, EEG signal, and eye blinking activities were detected in the experiments.

In the experiment, the face of the driver was also recorded by a video camera for calibration. The level of drowsiness was estimated based on the Wierwille and Ellsworth criteria [31] which were also adopted for driver drowsiness evaluation by Khushaba *et al.* [29]. The continuous scale included five descriptors: not drowsy (Class 1), slightly drowsy (Class 2), moderately drowsy (Class 3), very drowsy (Class 4), and extremely drowsy (Class 5) [31]. One-minute segment was evaluated by the scale as one of the five descriptors. In the evaluation pro-cess, two observers scored the drowsiness levels. The observers strictly followed the description of drowsiness as suggested by Wierwille and Ellsworth [31]. The full scale of the five descriptors was adopted, which means that one very alert segment was defined to be Class 1 and one very drowsy was defined to be Class 5. Most segments could reach an agreement. The disagreement occurred between adjacent classes in few cases. For example, one observer evaluated to be Class 1 and the other considered it as Class 2. This case did not affect the results as Classes 1 and 2 were both considered as alertness. Only in two cases, the observers could not reach an agreement for Classes 3 and 4. These two segments were not used in further analysis. To further avoid biasing judgment, we also used the "quantity" to verify the observation results as [37]. In the observation, the slow eyelid closures, rubbing the face or eyes, scratching, yawning, and nodding, were counted as drowsiness countermeasures. The number of the occurrence of the countermeasures determined the level of drowsiness. The results were allied to each other. In the test–retest examination, the results were similar. One segment considered as Class 5 was considered as Class 4. Another two segments evaluated as Class 2 were then considered to be Class 3. These Class 3 segments were removed for further analysis. Typical scoring results of morning and afternoon sessions are shown in Fig. 5.

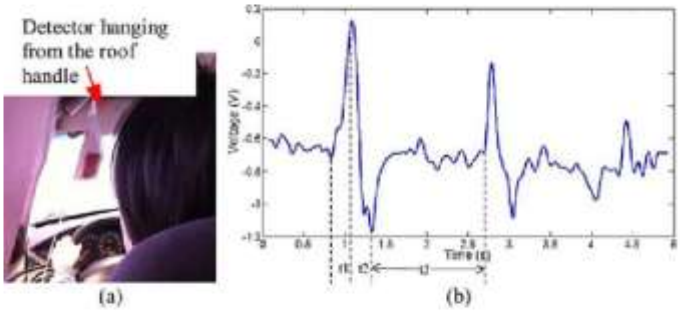

Fig. 6. Eye blinking detection. (a) Experiment protocol. (b) Typical signal detected from the system. *t*1, *t*2 are the eye closing time and the reopening time; *t*1+*t*2 is the overall blinking time; and *t*3 is the interval between blinking activities

C. Signal Preprocessing

The measured bio potential signal is contaminated with several sources of noise, such as electromyography (EMG), power line interference, electronic noise, and baseline drifts. The EMG signal is caused by human motion and muscle contraction, which typically ranges between 6 and 500 Hz [32]; the 60-Hz interference is due to the power line; and the drift is caused by the movement of electrode and breathing. The noise is filtered partially by the hardware filtering. A digital band pass filer was introduced to further reduce the noise. The four major bands of EEG signal ranges in 0–4, 4–8, 8–13, and 13–30 Hz, respectively. Therefore, the cut-off frequency of the digital filter was designed to be changeable. The pre-processed signals were then used in the subsequent analyses.

V. RESULT AND ANALYSIS

A. Vital Signal Measurement

1) Eye Blinking Detection:

A typical eye blinking signal is shown in fig. 6(b). The eye blinking activities cause pulses in the bio potential signals. Using peak identification algorithm developed in this paper, the occurrence of eye blinking can be determined in real time. Comparison study was conducted between the recorded signals and the video record. When the eyes started to close, a positive edge occurred immediately, whereas during reopening, negative edge followed. These formed a sharp pulse for one blinking cycle. Several key parameters can be analysed from the measured eye blinking signal in Fig 6(b), *t*1, *t*2 represents the eye closing time and reopening time.

Drowsy drivers typically have problems to control their eyes [13].Physiologically this behaves as rapid blinking at the on-set of drowsiness and slow blinking as the drivers are deeply affected.

2) EEG Detection:

Based on the raw EEG data detected from the system, the fast Fourier transform algorithm was applied to decompose the signal into four frequency bands. The detected wave components were compared with the standard clinic signals in order to evaluate the performance of the device Fig. 7(a)-(c) compared with waves, respectively. In each figure, the lower trace is the equal signal obtained from the nonintrusive system

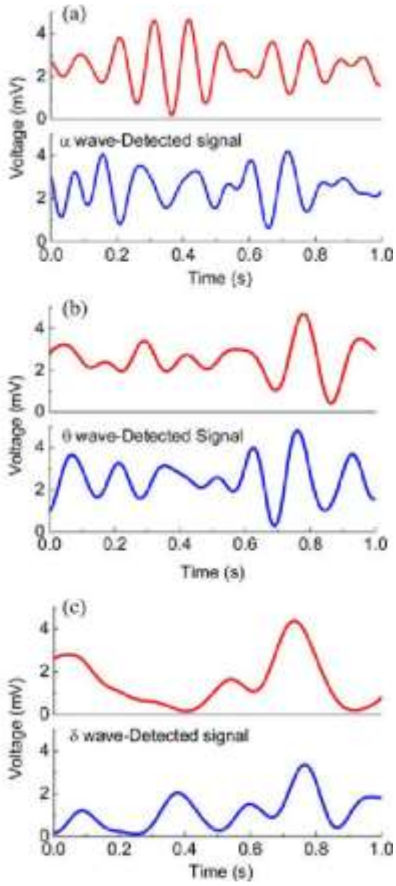

Fig. 7. EEG bands compared with clinic signals. (a) Alpha wave. (b) Theta wave. (c) Delta wave. In each figure, the upper trace is the typical EEG band signal and the lower one is that detected and computed by our system.

Whereas the upper one is the typical reference signals are allied to each other, which verify that the brain waves associated with EEG can be detected by the system.

3). *EEG Detection:*

The nonintrusive ECG measurement was verified by comparing with a clinic 12-lead ECG system. The clinic system .the clinic system used wet electrodes and electrolyte attached directly to the skin. Our electrode was placed right above the clinic electrode outside the cloth to compare the performance. A typical ECG signal detected from chest by our device is displayed as the lower trace in fig 8, whereas that detected from clinic chest lead is show as the upper trace. The two signals were detected simultaneously. In the capacitive ECG signal, R-R Intervals and QRS complexes are comparable to the clinic one. To detect HR and HRV automatically an algorithm was developed to pic the QRS peak and calculates the HR and HRV in real time. The HR HRV parameters including both time-domain and frequency-domain measures can be computed for further analysis.

B. System Stability in Driving Scenarios

During normal driving drivers, drivers stay still in most of time. However at some time the movements and friction between the electrode and human body can cause severe motion

TABLE I

STABILITY OF THE PERFORMANCE DURING DIFFERENT SCENARIOS

Scenarios	QRS	Eye blinking pulse		EEG
		Roof	Glasses	
Highway	100%	15%	90%	80%
Urban	95%	35%	75%	35%
Turning	95%	5%	85%	15%
Urban (Attention)	100%	75%	90%	85%

Artefact's for CEs. Therefore, it is needed to analyse the feasibility of applying the nonintrusive system in automobile applications. From implementation perspective, however, it is not necessary for a perfect signal at every second during driving [1]. For example, for each 1-min segment, if the detected signal can be stable for more than 15 s, this segment can be considered as a successful one. The stability of the system is defined as the number of successful segments over total number of segments. The results from a typical subject are shown in Table I (total 20 segments were analysed).

From Table I, it can be seen that the performance for HR and HRV detection is reasonably stable, which qualifies the function for long-term application. The performance for eye activity detection is unsatisfactory when the electrode is mounted on the roof. The performance, however, is significantly improved when placed on the glasses frame. In the data collection process, the electrodes made of soft metal taps were placed wrapped on the frame of the eyeglasses. They could be bended and attached. It is also found that in highway scenarios where drivers have less motion, the system performance demonstrates high stability. Under a traffic condition, where more motions are involved in vehicle operation, the results are still acceptable in most cases. It is also noticed during the experiments that when the drivers were asked to reduce their motion, the recorded signals became more stable.

C. Fatigue Detection Background

A few physiological parameters of drivers have been observed to be well connected to drowsiness. In the eye-activity-based assessment, one of the most widely used parameters is the PERCLOS which refers to the duration of eye closure over 80% of time [13]. Other parameters such as reopening time [7], the intervals between eye blinks, and the speed of blinking [8] were also studied by some researchers.

In EEG-based assessment, Lal *et al*. [9] developed an algorithm to assess driver drowsiness based on the changes in EEG bands (α, ϑ, β, and δ bands). Lin *et al*. [10] estimated the drowsiness level by independent component analysis (ICA) of EEG and found the optimal locations to place EEG electrodes. Jap *et al*. [33] compared four algorithms based on the four EEG and found the optimal locations to place EEG electrodes. Jap *et al*. [33] compared four algorithms based on the four EEG bands. The result showed that a slight decrease of alpha activity and a significant decrease of beta activity were associated with fatigue. The ECG features are also extracted to analyse sleepiness, including both time domain and frequency domain. Yang *et al*. [34] classified sleep into wake, rapid eye movement (REM) and non-REM stages using very low frequency (VLF), low frequency (LF), high frequency (HF) and the LF/HF ratio in HRV analysis. Roman *et al*. [8] used defriended fluctuation analysis and observed some scaling differences between sleep deprived and no deprived groups.

D. Feature Extraction

In this study, we also extracted and analysed the features from the three types of vital signals. For eye activities, the blinking frequency (blinking times per min), blink duration [$t1+t2$ in Fig. 6(b)] were adopted as the measures of eye blinking activities. For EEG signals, first, two digital band pass filters with the pass band ranging in 8–13 Hz and 13–30 Hz were applied to the data to extract the alpha wave and beta wave from the original signals. Then power density of the two waves was calculated to compare the alertness and sleepiness conditions of each subject. For ECG signal, HRV and its selected measures in time domain and frequency domain were selected and calculated as described in Table II.

To differentiate driver states, Classes 1 and 2 were marked as alertness and Classes 4 and 5 were marked as drowsiness in the data analyses. One-way ANOVA was applied to test the significance of each feature.

E. Result and Discussion for Fatigue Detection Application

1) Eye Blinking Results: In the alertness condition, the average blinking frequency of the 12 subjects was 7.0 ± 1.6 times per minute; the average blinking duration was around

11.3 ms. In the Class 4 drowsiness condition, two of the subjects blinked faster than in the alertness condition; the rest were similar. The average blinking frequency of the subjects was 8.2 ± 3.0 times per minute. In the Class 5 drowsiness condition, the eyelid began to close slowly acting as the duration of each blinking activities

Becoming much longer. The blinking duration shows the significance between alertness and extremely drowsiness (p <0.05). All the results are illustrated in Table III.

2). EEG Results: Two of the EEG results were not feasible for data analysis as the electrodes slipped away from the hair in the experiment. The rest ten groups of data were used for feature extraction. Comparing the EEG signals in alertness and fatigue conditions of each subject, the alpha wave decreased slightly while the beta wave remained relatively stable. This result is analogous to that in [33]. However, the ANOVA analysis did not show the significant linkage of either alpha or beta waves with extent of drowsiness

HRV Results: In the time domain, the SDNN and RMSSD (described in Table II) are two main statistical measures of HRV. From the results, little change can be found from the SDNN and RMSSD, which means that the HR did not show significant difference between the alertness and sleepiness conditions. In the frequency domain, the spectral power density of LF, HF, and the ratio of LF/HF were extracted from the HRV data. The power density of LF component remained similar in the two condition, whereas the FF component remained similarly in the two conditions , whereas the HF increased apparently from alertness to drowsiness. The power density of HF and the ratio of LF/HF are significant measures to distinguish alertness and drowsiness. This result is similar to that observation [12]

VI. DISCUSSION AND CONCLUSION

In this paper, we developed an innovative non-invasive driver assistance system. The system features high sensitivity in the measurement of bio potentials on human body and requires no physical contact with skin. This method causes less mental or physical loads to the drivers and is advantageous for long-term driver monitoring purpose. The system can measure physiological signals such as eye blinking activity, EEG and ECG signals in the real time, which are widely accepted vital signals for health monitoring and drowsiness measures. The performance of the system was verified on a high-fidelity driving simulator. Experiments were conducted on subjects with different alert-ness and sleepiness conditions. The eye activity, EEG and ECG features were recorded on the alert and drowsy drivers using the nonintrusive system. Results showed that the blinking duration, and the LF, HF components from HRV are significant physio-logical measures between alertness and drowsiness, which are consistent with other studies. Our long-term goal is to develop this technology into a robust in-vehicle driver diagnosis and medical assistance system to improve the health and safety of drivers.

REFERENCES

- T. Wartzek, B. Eilebrecht, J. Lem, H.-J. Lindner, S. Leonhardt, and M. Walter, "ECG on the road: Robust and unobtrusive estimation of heart rate," *IEEE Trans. Biomed. Eng.*, vol. 58, no. 11, pp. 3112–3120, Nov. 2011.
- A. H. Taylor and L. Dorn, "Stress, fatigue, health and risk of road traffic accidents among professional drivers: The contribution of physical inactivity," *Annu. Rev. Public Health*, vol. 27, pp. 371–391, 2006.
- L. Copeland, "Study: Sleepiness a factor in 17% of road deaths," *USAToday*, Nov. 8, 2010.
- Y. Dong, Z. Hu, K. Uchimura, and N. Murayama, "Driver inattention monitoring system for intelligent vehicles: A review," *IEEE Trans. Intell.Transp.*, vol. 12, no. 2, pp. 596–614, Jun. 2011.
- Y. M. Chi, T.-P. Jung, and G. Cauwenberghs, "Dry-contact and noncontact biopotential electrodes: Methodological review," *IEEE Rev. Biomed. Eng.*, vol. 3, pp. 106–119, 2010.
- S. K. L. Lal and A. Craig, "A critical review of the psychophysiology of driver fatigue," *Biol. Psychol.*, vol. 55, pp. 173–194, 2001.
- P. P. Caffier, U. Erdmann, and P. Ullsperger, "Experimental evaluation of eye-blink parameters as a drowsiness measure," *Eur. J. Appl. Physiol.*, vol. 89, pp. 319–325, 2003.
- B. Roman, S. Pavel, P. Miroslav, V. Petr, and P. Lubomir, "Fatigue Indicators of drowsy drivers based on analysis of physiological signals," in *Proc. 2nd Int. Symp. Med. Data Anal.*, 2001, pp. 62–68.
- C. T. Lin, R. C. Wu, S. F. Liang, W. H. Chao, Y.-J. Chen, and T.-P. Jung, "EEG-based drowsiness estimation for safety driving using independent component analysis," *IEEE Trans. Circuits Syst. I, Reg. Papers*, vol. 52, no. 12, pp. 2726–2738, Dec. 2005.
- Y. G. Lim, K. K. Kim, and K. S. Park, "ECG recording on a bed during sleep without direct skin-contact," *IEEE Trans. Biomed. Eng.*, vol. 54, no. 4, pp. 718–725, Apr. 2007.
- A. Aleksandrowicz and S. Leonhardt, "Wireless and non-contact ECG measurement system—The Aachen Smart Chair," *Acta Polytechnica*, vol. 2, pp. 68–71, 2007.
- G. Yang, Y. Lin, and P. Bhattacharya, "A driver fatigue recognition model based on information fusion and dynamic Bayesian network," *Inform.Sci.*, vol. 180, pp. 1942–1954, 2014.
- B. T. Jap, S. Lal, P. Fischer, and E. Bekiaris, "Using EEG spectral components to assess algorithms for detecting fatigue," *Expert Syst. Appl.*, vol. 36, pp. 2352–2359, 2009.
- A. B. Barreto, S. D. Scargle, and M. Adjouadi, "A practical EMG-based human-computer interface for users with motor disabilities," *J. Rehabil.Res. Dev.*, vol. 37, pp. 53–64, 2000.
- R. N. Khushaba, S. Kodagoda, S. Lal, and G. Dissanayake, "Driver drowsiness classification using fuzzy wavelet-packet-based feature-extraction algorithm," *IEEE Trans. Biomed. Eng.*, vol. 58, no. 1, pp. 121–131, Jan. 2012.
- G. D. Gargiulo, A. L. McEwan, P. Bifulco, M. Cesarelli, C. Jin, J. Tapson, A. Thiagalingam, and A. Van Schaik, "Towards true unipolar bio-potential recording: A preliminary result for ECG," *Physiol. Meas.*, vol. 34, pp. N1– N7, 2013.

